

Mixed Convection MHD Flow of a Nanofluid in a Rotating System with Heat Generation/Absorption



P. Vimala and K. Manimegalai

1 Introduction

Stretching sheet phenomenon has many real-life applications in industrial areas such as extrusion, glass blowing, production of papers, manufacture of plastics and spinning of fibers. These applications involve enormous heat and mass transfer. Therefore, many investigations on such flows have been carried out to study the heat and mass transfer characteristics [1–5]. [1] investigated the flow past a linear stretching plate with heat conduction. [2] studied the suction and injection flow of a viscous fluid in a porous stretching sheet with heat and mass transfer. [3] studied the heat transfer characteristics of electrically conducting fluid flow between two horizontal plates with stretching and porosity. [4] investigated the flow of a viscous incompressible fluid over a continuous stretching sheet with heat transfer characteristics. [5] obtained a numerical solution of free convection flow over a porous stretching sheet.

In the above investigations, rotation phenomenon has not been considered. However, this phenomenon is encountered in many practical applications such as rotating machinery and cooling processes. Owing to the significance of rotational geometries in many industries, [6] studied electrically conducting fluid flow over a stretching sheet in a porous rotating geometry.

All the above papers considered flow of viscous incompressible fluids. However, in many applications such as cooling processes in machines, heat exchangers and chemical processing, nanofluids are used owing to their better heat transfer characteristics. Nanofluids are high thermal conducting particle suspensions in low thermal conducting base fluids. Such fluids have higher thermal conductivity when compared to their base fluids. This property of nanofluids makes them more significant in applications involving enormous heat transfer. Hence, [7] adopted a homogeneous flow model with conventional transport equations for pure fluids along with the physical properties of nanofluids. [8] analyzed the flow and heat transfer of copper–water

P. Vimala (✉) · K. Manimegalai

Department of Mathematics, Anna University, Chennai, India

nanofluid between stretching and porous surfaces using HAM in a rotating system. The above articles [7, 8] used a single-phase model for the study of nanofluid flow. These studies showed the enhancement of heat transfer characteristics of nanofluids significantly.

Introduced by [9], a two-phase model has also been used in the literature [10] for describing the flow behavior of nanofluids. [9] presented seven slip mechanisms between nanoparticles and base fluids. [10] studied the nanofluid flow and heat transfer in a rotating system using numerical method.

Although many investigations have been carried out in flow of nanofluids between parallel plates, factors such as mixed convection flow in such geometries, presence of internal heat source/sink and presence of a magnetic field may impact the flow behavior as well as the heat and mass transfer characteristics. Therefore, the present problem discusses a mixed convection steady MHD flow of a nanofluid between a lower stretching plate and an upper porous plate in a rotating system. Further, the flow is assumed to have an internal heat source/sink. The governing equations are derived using two-phase model, and the formulation is presented in Section II. The problem is then solved using SAM as in Section III. Section IV presents the results with appropriate graphical representations. Section V gives the conclusion.

2 Mathematical Formulation

A mixed convection steady laminar flow of an incompressible nanofluid between two horizontal parallel circular plates is considered as shown in Fig. 1. The lower plate is stretched along its plane by equal and opposite forces keeping the origin unchanged. The upper plate is porous and is at a distance of $h(t)$ from the lower plate. Fluid flows through the pores in the upper plate with a constant wall suction/injection velocity

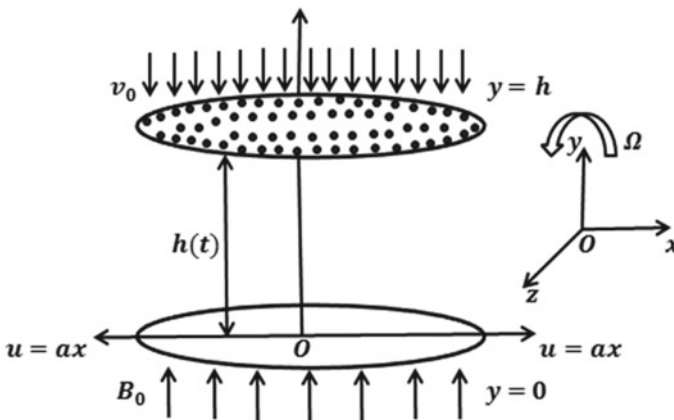


Fig. 1 The flow geometry

v_0 . Both the plates rotate with a constant angular velocity Ω about the y -axis, which makes the nanofluid between them to rotate, and there is net cross flow along the z -axis. A uniform magnetic field of intensity B_0 is applied in the direction of the y -axis. It is assumed that there is an internal heat source/sink with heat generation/absorption parameter Q_0 . Under these conditions, the nondimensional form of the governing equations of the nanofluid MHD mixed convection flow along with heat source/sink is given by

$$\begin{aligned} &(-h^2/\alpha x \rho_f \nu)(\partial P^*/\partial x) \\ &= -[f''' - R(f'^2 - ff'') - 2Krg - Mf' + Gr_t\theta + Gr_c\phi] \end{aligned} \tag{1}$$

$$(-1/\rho_f h)(\partial P^*/\partial \eta) = a^2 h(ff' + f''/R) \tag{2}$$

$$g'' - R(f'g - fg') + 2Krf' - Mg = 0 \tag{3}$$

$$\theta'' + Pr(Rf\theta' + Nb\theta'\phi' + Nt\theta^2 + Q\theta) = 0 \tag{4}$$

$$\phi'' + (Nt/Nb)\theta'' + RScf\phi' = 0 \tag{5}$$

where the following nondimensional variables have been used

$$\eta = \frac{y}{h(t)}, u = \alpha x f'(\eta), v = -ahf(\eta), w = \alpha x g(\eta), \theta = \frac{T - T_h}{T_0 - T_h}, \phi = \frac{C - C_h}{C_0 - C_h} \tag{6}$$

where u, v and w denote the fluid velocity components in the x, y and z directions, respectively, p^* is the modified fluid pressure, T is the temperature of the fluid, T_h is the temperature at the upper plate and ρ_f, ν and α are the fluid density, kinematic viscosity and thermal diffusivity, respectively. Also, C is the concentration of the nanoparticles, D_T is the thermophoretic diffusion parameter, D_B is the Brownian motion coefficient, $(\rho c_p)_p/(\rho c_p)_f$ is the ratio of effective heat capacity of the nanoparticle to the heat capacity of the fluid, g is the magnitude of acceleration due to gravity, β_T is the thermal expansion coefficient, β_C is the concentration expansion coefficient, and Q_0 is the uniform volumetric heat generation ($Q_0 > 0$) or absorption ($Q_0 < 0$) parameter. $R = ah^2/\nu$ is the Reynolds number, $Kr = \Omega h^2/\nu$ is the rotational number, $M = \sigma B_0^2 h^2/\nu \rho_f$ is the magnetic parameter or Hartmann number, $Gr_t = \tilde{g} \beta_T h^2 (T_0 - T_h) \alpha x = Gr \backslash Re_x^2$ is the ratio between the modified Grashof number Gr and square of the local Reynolds number Re_x , which represents the temperature mixed convection parameter, $Gr_c = \tilde{g} \beta_C h^2 (C_0 - C_h) \alpha x$ represents the concentration mixed convection parameter, $Pr = \mu c_p/k$ is the Prandtl number, $Q = Q_0 h^2/(\rho c_p)_f \nu$ is the heat source/sink parameter, $Sc = \nu/D_B$ is the Schmidt number,

$Nb = (\rho c_\rho)_p D_B(C_0 - C_h)/(\rho c_\rho)_f \nu$ is the Brownian motion parameter, and $NT = (\rho c_\rho)_p D_T(T_0 - T_h)/(\rho c_\rho)_f \nu$ is the thermophoresis parameter.

Eliminating the pressure gradient terms, Eqs. (1) and (2) yield

$$f'''' - R(f' f'' - f f''') - 2Krg' - Mf'' + Gr_t \theta' + Gr_c \phi' = 0 \tag{7}$$

Thus, it is required to solve the governing equations Eqs. (3)-(5) and (7) of the present problem with the boundary conditions

$$f'(0) = 1, f(0) = 0, g(0) = 0, \theta(0) = 1, \phi(0) = 1 \tag{8}$$

$$f'(1) = 0, f(1) = \lambda, g(1) = 0, \theta(1) = 0, \phi(1) = 0 \tag{9}$$

where $\lambda = v_0/ah$ is the porosity parameter.

3 Solution by SAM

Expanding the unknown variables f, g, θ and ϕ in powers of R which is of the order $O(1)$, (as in [11, 12])

$$\begin{aligned} f(\eta) &= f_0 + Rf_1 + R^2 f_2 + O(R^3) \\ g(\eta) &= g_0 + Rg_1 + R^2 g_2 + O(R^3) \\ \theta(\eta) &= \theta_0 + R\theta_1 + R^2 \theta_2 + O(R^3) \\ \phi(\eta) &= \phi_0 + R\phi_1 + R^2 \phi_2 + O(R^3) \end{aligned} \tag{10}$$

and substituting Eq. (10) in the reduced governing Eqs. (3)-(7) and the boundary conditions (8) and (9), the final equations are solved for $f(\eta), g(\eta), \theta(\eta)$ and $\phi(\eta)$ upto the second order approximation.

The zeroth-order solutions are

$$f_0(\eta) = A_0 \eta^3 + B_0 \eta^2 + \eta, g_0(\eta) = 0, \theta_0(\eta) = 1 - \eta, \phi_0(\eta) = 1 - \eta, .$$

where $A_0 = 1 - 2\lambda, B_0 = 3\lambda - 2$.

The first-order solutions are

$$f_1(\eta) = \frac{A_1 \eta^7}{840} + \frac{B_1 \eta^6}{360} + \frac{C_1 \eta^5}{120} + \frac{D_1 \eta^4}{24} + \frac{E_1 \eta^3}{6} + \frac{F_1 \eta^2}{2}, .$$

$$g_1(\eta) = -\frac{2Kr}{R} \left(\frac{A_0 \eta^4}{4} + \frac{B_0 \eta^3}{3} + \frac{\eta^2}{2} - G_1 \eta \right), .$$

$$\theta_1(\eta) = Pr \left(\frac{A_0 \eta^5}{20} + \frac{B_0 \eta^4}{12} + \frac{H_1 \eta^3}{6} - \frac{I_1 \eta^2}{2} - J_1 \eta \right),$$

$$\phi_1(\eta) = Le \left(\frac{A_0 \eta^5}{20} + \frac{B_0 \eta^4}{12} + \frac{\eta^3}{6} - k_1 \eta \right),$$

where $A_1, B_1, C_1, D_1, E_1, F_1, G_1, H_1, I_1, J_1$ and K_1 .

$$A_1 = 48\lambda^2 - 48\lambda + 12, B_1 = -72\lambda^2 + 84\lambda - 24, D_1 = 2B_0 \left(1 + \frac{M}{R} \right) + \frac{Gr_t}{R} + \frac{Gr_c}{R},$$

$$E_1 = -\frac{A_1}{28} - \frac{B_1}{15} - \frac{3C_1}{20} - \frac{D_1}{2}, F_1 = \frac{A_1}{105} + \frac{B_1}{60} + \frac{C_1}{30} + \frac{D_1}{12}, G_1 = \frac{A_0}{4} + \frac{B_0}{3} + \frac{1}{2},$$

$$H_1 = 1 + \frac{Q}{RPr}, I_1 = \frac{Nb + Nt + Q}{R},$$

$$J_1 = \frac{A_0}{20} + \frac{B_0}{12} + \frac{H_1}{6} - \frac{I_1}{2} \text{ and } K_1 = \frac{A_0}{20} + \frac{B_0}{12} + \frac{1}{6}.$$

The second-order expressions are very lengthy, and hence, they are not presented here. However, solutions upto second order have been obtained and presented in the graphical representations. Using the zeroth-order, first-order and second-order solutions in Eq. (10), approximate expressions upto second order for the flow variables $f(\eta)$ and $g(\eta)$, temperature distribution $\theta(\eta)$ and concentration distribution $\phi(\eta)$ can be obtained.

4 Results and Discussion

The steady MHD rotating flow of an incompressible nanofluid between a lower stretching plate and an upper porous plate is studied. Using SAM, the problem is solved, and the effects of various parameters on velocity, temperature and concentration distributions are discussed. Further, a comparison of the present results is made with those of the existing literature. As the flow is considered to be laminar and between parallel plates, the value of the Reynolds number R is taken as 1. The values of the rotation number Kr and magnetic Hartmann number M are chosen to be 1 each. Since mixed convection is considered, the values of temperature Grashof number Gr_t and concentration Grashof number Gr_c are chosen to be equal to 1 each. As the nanoparticle size is very small, the values of Brownian motion parameter Nb , thermophoresis parameter Nt and Schmidt number Sc are taken to be equal to 0.1 each. Prandtl number Pr of water is 6.2. The value of heat generation/absorption value Q due to the internal source/sink is taken as 0.3. The above values of the parameters are used in obtaining the results, unless otherwise specified.

Figures 2 and 3 compare the present results when $M = 0, Gr_t = 0, Gr_c = 0, Q = 0$ with those of [8]. Here, Φ represents the volume fraction of [8]. Figure 2 shows the effects of the porosity parameter λ and Reynolds number R on the temperature distribution $\theta(\eta)$. It is seen that an increase in the porosity parameter results in a decrease in temperature distribution and an increase in Reynolds number results in a further decrease in temperature distribution. On neglecting the Brownian motion and thermophoresis effects (ie. $Nb = Nt = 0$) and the Schmidt number ($Sc = 0$), the present results agree well with [8]. Further, the present results including these effects ($Nb = Nt = 0.1$ and $Sc = 0.1$) show an enhanced temperature distribution. Figure 3 shows a comparison of temperature distribution $\theta(\eta)$ between single-phase model [8] and two-phase model of the present work. It is observed from the results of [8] that as the volume fraction Φ increases, temperature distribution increases.

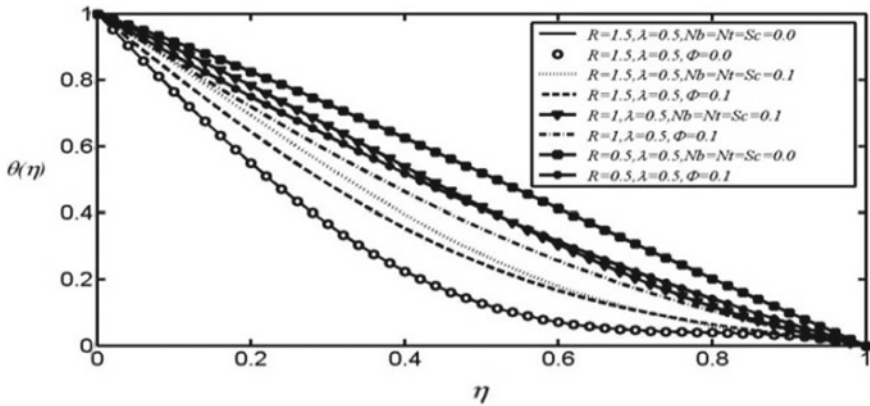


Fig. 2 Effects of porosity parameters and Reynolds number on temperature distribution—A comparison

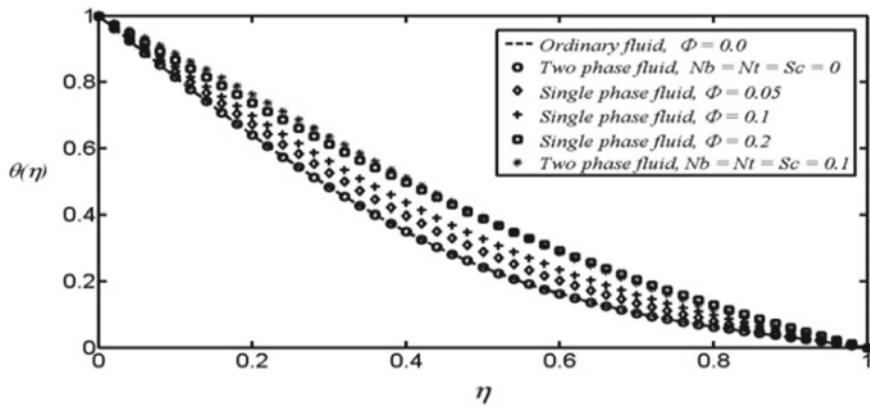


Fig. 3 Comparison of the single-phase (Sheikholeslami [8]) and two-phase models (present model) $R = 0.5, Kr = 0.5, Gr_t = 1, Gr_c = 1, M = 1, Pr = 6.2, Q = 0.3$

Also, a further increase in temperature distribution is observed in the present work due to the effects of Brownian motion Nb , thermophoresis Nt and Schmidt number Sc .

In Fig. 4a, x -direction velocity component $f'(\eta)$ has a dual behavior. In the first half ($0 \leq \eta \leq 0.5$) of the region, y -direction velocity component $f'(\eta)$ increases with temperature Grashof number Gr_t while in the second half ($0.6 \leq \eta \leq 1$), $f'(\eta)$ increases in the negative direction with temperature Grashof number. From Fig. 4b, it is seen that y -direction velocity component $f(\eta)$ increases with an increase in temperature Grashof number. Distribution of z -direction velocity component $g(\eta)$ (Fig. 4c) is similar to that of x -direction velocity component (Fig. 4a). As temperature Grashof number increases, the temperature distribution decreases as seen in Fig. 4d.

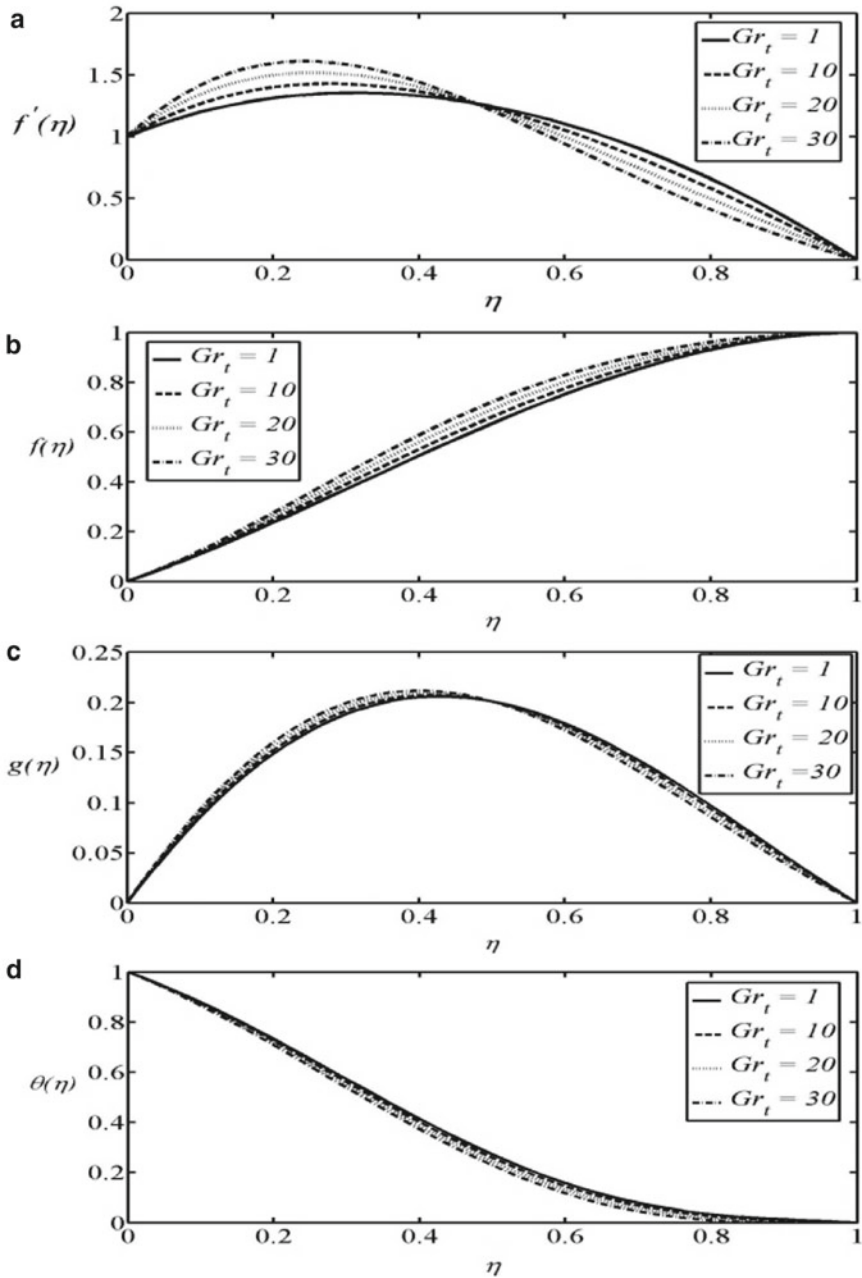


Fig. 4 Effects of temperature Grashof number on the velocity components (a, b, c) and temperature distribution (d)

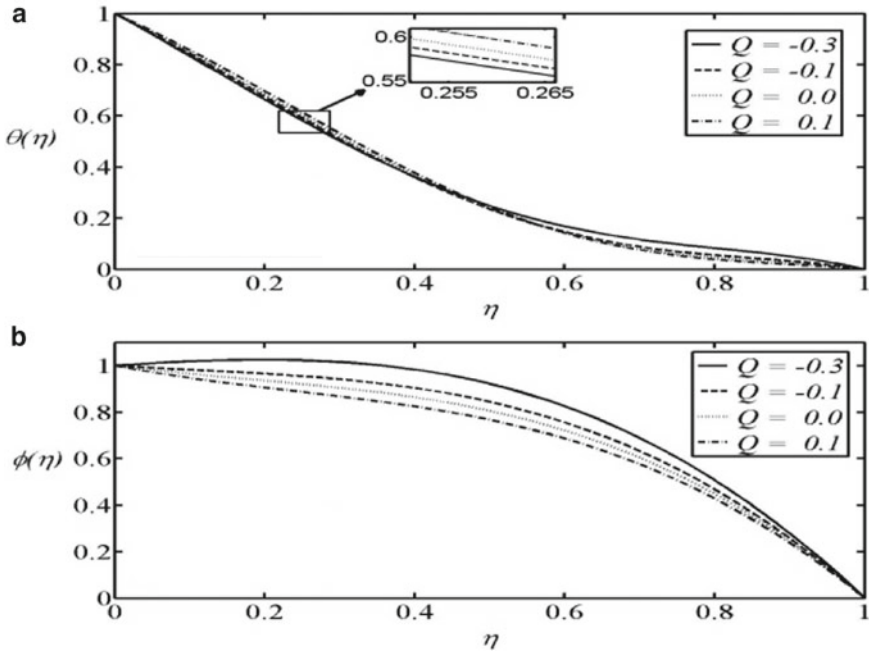


Fig. 5 Effects of heat source/sink parameters on the temperature distribution (a) and concentration distribution (b)

The effect of temperature Grashof number on concentration distribution $\phi(\eta)$ is negligible. Gr_c

Figure 5 presents the effects of heat generation/absorption parameter Q . $Q > 0$ represents the heat source or heat generation causing temperature ($\theta(\eta)$) enhancement, whereas $Q < 0$ represents the heat sink or heat absorption which reduces the temperature distribution $\theta(\eta)$. In Fig. 5a, temperature distribution increases for greater values of heat generation/absorption parameter from lower part to middle of the channel, but the trend is reversed in the upper half of the channel due to the porosity of the upper plate. In Fig. 5b, concentration distribution $\phi(\eta)$ decreases with an increase in heat generation/absorption parameter.

5 Conclusions

An investigation of the mixed convection steady laminar flow of an incompressible nanofluid between a stretching sheet and a porous plate is carried out considering a two-phase model. The problem is solved by SAM. It is seen that mixed convection flow of nanofluid enhances the heat transfer characteristics, heat source/ sink improves the temperature distribution in the nanofluid.

References

1. Crane LJ (1970) Flow past a stretching plate. *Z Angew Math Phys* 21:645–647
2. Gupta PS, Gupta AS (1977) Heat and mass transfer on a stretching sheet with suction or blowing. *Can J Che Eng* 55(6):744–746
3. Borkakoti AK, Bharali A (1983) Hydromagnetic flow and heat transfer between two horizontal plates, the lower plate being stretching sheet. *Q Appl Math* 41:461–467
4. Chen CK, Char MI (1988) Heat transfer of a continuous, stretching surface with suction or blowing. *J Math Ana App* 135:568–580
5. Vajravelu K (1994) Convection heat transfer at a stretching sheet with suction or blowing. *J Math Anal Appl* 188:1002–1011
6. Vajravelu K, Kumar BVR (2004) Analytical and numerical solutions of a coupled non-linear system arising in a three-dimensional rotating flow. *Int J Non-Linear Mech* 39:13–24
7. Choi SUS, Eastman JA (1995) Enhancing thermal conductivity of fluids with nanoparticles. *ASME Int Mech Eng Con Exp* 231:99–105
8. Sheikholeslami M, Ashorynejad HR, Domairry G, Hashim I (2012) Flow and heat transfer of Cu-water nanofluid between a stretching sheet and a porous surface in a rotating system. *J Appl Math* 2012:1–18
9. Buongiorno J (2006) Convective transport in nanofluids. *Trans ASME* 128:240–250
10. Sheikholeslami M, Ganji DD (2014) Numerical investigation for two-phase modeling of nanofluid in a rotating system with permeable sheet. *J Mol Liquids* 194:13–19
11. Usha R, Vasudevan S (1993) A similar flow between two rotating disks in the presence of a magnetic field. *J Appl Phys* 60:707–714
12. Usha R, Vimala P (1998) Magheto-hydrodynamic disk braking. *Z Angew Math Mech* 4:283–288